Choosing Suitable Shielding Gas for Thermal Optimization of GTAW Process

A.MOARREFZADEH
Mechanical Engineering Group Department
Mahshahr Islamic Azad University
Mahshahr
IRAN
a_moarrefzadeh@yahoo.com

Abstract: Thermal effects of Gas Tungsten Arc (GTA) and temperature field from it on workpiece (copper) and shielding gas type, is the main key of process optimization for GTAW. Energy source properties of GTA strongly depend on physical property of a shielding gas. In this paper, carbon dioxide (CO_2) was used as an alternative gas for its low cost. The basic energy source properties of CO_2 GTA were numerically predicted ignoring the oxidation of the electrodes. It was predicted that CO_2 GTA would have excellent energy source properties comparable to that of He, Ar GTA.

Key-Words: Numerical simulation, Tungsten, Copper, Shielding gas, Argon, Helium, CO_2, GTAW

1 Introduction

The necessary heat for Gas Tungsten Arc Welding (TIG) is produced by an electric arc maintained between a nonconsumable tungsten electrode and the part to be welded.

The heat-affected zone, the molten metal, and the tungsten electrode are all shielded from the atmosphere by a blanket of inert gas fed through the GTAW torch. Inert gas is that which is inactive, or deficient in active chemical properties. The shielding gas serves to blanket the weld and exclude the active properties in the surrounding air. It does not burn, and adds nothing to or takes anything from the metal. Inert gases such as Carbon dioxide and argon and helium do not chemically react or combine with other gases. They possess no odor and are transparent, permitting the welder maximum visibility of the arc. In some instances a small amount of reactive gas such as hydrogen can be added to enhance travel speeds.

The GTAW process can produce temperatures of up to 35,000° F/ 19,426° C. The torch contributes only heat to the workpiece. If filler metal is required to make the weld, it may be added manually in the same manner as it is added in the oxyacetylene welding process. There are also a number of filler metal feeding systems available to accomplish the task automatically. Fig.1.a shows the essentials of the manual GTAW process. Also Fig.2.b shows the Simultaneous imaging of weld pool and keyhole.

The greatest advantage of the GTAW process is that it will weld more kinds of metals and metal alloys than any other arc welding process. TIG can be used to weld most steels including stainless steel, nickel alloys, titanium, aluminum, magnesium, copper, brass, bronze, and even gold. GTAW can also weld dissimilar metals to one another such as copper to brass and stainless to mild steel.

The concentrated nature of the GTAW arc permits pin point control of heat input to the workpiece resulting in a narrow heat-affected zone.
A high concentration of heat is an advantage when welding metals with high heat conductivity such as aluminum and copper. A narrow heat-affected zone is an advantage because this is where the base metal has undergone a change due to the superheating of the arc and fast cooling rate. The heat-affected zone is where the welded joint is weakest and is the area along the edge of a properly made weld that would be expected to break under a destructive test.

Thermal effects of welding electrical arc and thermal field from it on workpiece(copper) and shielding gas type, is the main key of analysis and process optimization for GTAW, that main goal of this paper is defined about that.

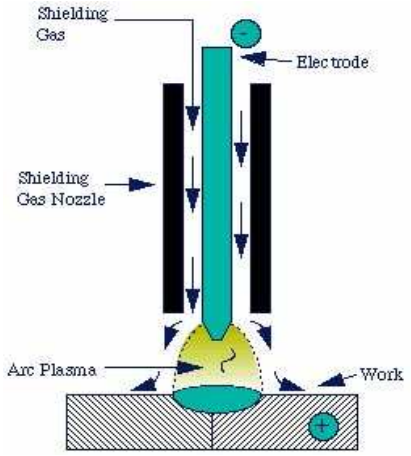

Fig.1.a. Nozzle GTAW process[1]

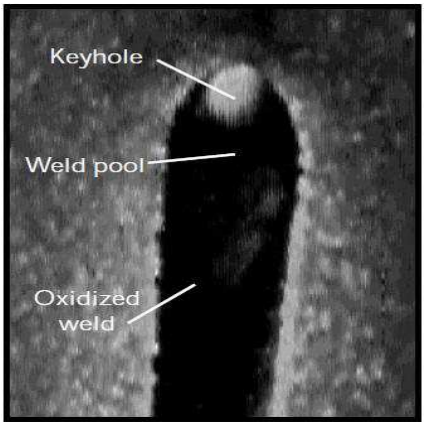

Fig.1.2. Simultaneous imaging of weld pool and keyhole[1]

Welding process numerical simulation and effective parameters on it with Ansys software finding the thermal field material, the effect of parameters variation on thermal field by considering shielding gases Ar,He,CO_2 and finally discussion about this process to being optimization are the main parts of this paper.

In this paper, by adopting carbon dioxide (CO_2), the basic energy source properties of CO_2 GTA are predicted. The properties of arc plasma and heat input intensity to a water-cooled copper anode are numerically analyzed ignoring oxidation of electrodes. The results are compared with those of conventional argon (Ar) and He GTA.[1]

2 Numerical simulation

This process simulation using the thermal transient analysis in Ansys software by SIMPLE numerical method in a exact way and considering separated fields for cooper, as a workpiece and shielding gas in 3 cases, Ar, He, CO_2 and a field for air around them starts. The equations of these fields are derived and at the end by thermal loading, equations of different fields are solved. The derived answers of thermal fields, the effect of each welding parameters are thus we can receive the GTAW process optimization. All mention steps for all 3 shielding gases happen till the thermal effect of each of them are achieved completely for the process optimization.

As interface equations of fluid and solid are non linear, analytical solutions are almost useless, because with inputs and initial values that give to interface problems to solve them, the problem gets so complicated , and numerical techniques are the only ways that we have for finding complete solutions.[3]

Finite elements simulations are done in 3 steps with the main pieces :

1- Modeling by FEMB

2- The thermal study and processing

3-Post-Processing result of analysis by Ansys software for results discussion

Modeling special technics for a finite elements :

1- Finite elements modeling , types and properties for model different parts
2- The definition of material properties
3- parameter definition
4- Loading
5- Boundary and initial value definition
6- Common interfaces definition
7- Control parameter definition

2.1 Finite element modeling

In Fig.2, finite element model is shown For meshing of solid field (copper) by considering the study of thermal field, from the thermal elements set, we chose the PLANE55 type. Because as axisymmetric element with conduction property, this element has 4 node with one degree of freedom. This element has mesh moving property as well. For shielding gas in 3 mentioned steps use FLUID141 element. Because this element is so suitable for transient thermal modeling. Also this element has thermal energy transmitting property.

2.2 Arc-electrode model

The tungsten cathode, arc plasma and anode are described in a frame of cylindrical coordinate with axial symmetry around the arc axis. The calculation domain is shown in Fig. 3. The diameter of the tungsten cathode is 3.2mm with a 60° conical tip. The anode is a water-cooled copper. The arc current is set to be 150 A. Ar, He or CO_2 is introduced from the upper boundary of the calculation domain. The flow is assumed to be laminar, and the arc plasma is assumed to be under local thermodynamic equilibrium (LTE). Physical properties of shielding gases are calculated in the same manner as that in literature .
The dependences of specific heat, thermal conductivity and electrical conductivity of the gases on the temperature are shown in Fig. 4.
The differential Eqs. (1)–(8) are solved iteratively by the SIMPLEC numerical procedure:

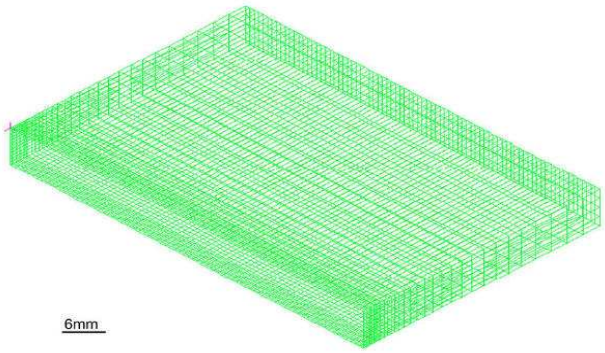

Fig.2. Modeling and Meshing[2]

Mass continuity equation:

$$\frac{1}{r}\frac{\partial}{\partial r}(r\rho v_r)+\frac{\partial}{\partial z}(\rho v_z)=0 \qquad (1)$$

Radial momentum conservation equation:

$$\frac{1}{r}\frac{\partial}{\partial r}(r\rho v_r^2)+\frac{\partial}{\partial z}(\rho v_r v_z)= -\frac{\partial \rho}{\partial r}-j_z B_\theta+\frac{1}{r}\frac{\partial}{\partial r}(2r\eta\frac{\partial v_r}{\partial r}) +\frac{\partial}{\partial z}(\eta\frac{\partial v_r}{\partial z}+\eta\frac{\partial v_z}{\partial r})-2\eta\frac{v_r}{r^2}. \qquad (2)$$

Axial momentum conservation equation:

$$\frac{1}{r}\frac{\partial}{\partial r}(r\rho v_r v_z)+\frac{\partial}{\partial z}(\rho v_z^2)= -\frac{\partial \rho}{\partial z}+j_r B_\theta+\frac{\partial}{\partial z}(2\eta\frac{\partial v_z}{\partial z})+ \frac{1}{r}\frac{\partial}{\partial r}(r\eta\frac{\partial v_r}{\partial z}+r\eta\frac{\partial v_z}{\partial r}). \qquad (3)$$

Energy conservation equation:

$$\frac{1}{r}\frac{\partial}{\partial r}(r\rho v_r h)+\frac{\partial}{\partial z}(\rho v_z h)= \frac{1}{r}\frac{\partial}{\partial r}(\frac{rk}{c_p}\frac{\partial h}{\partial r})+\frac{\partial}{\partial z}(\frac{k}{c_p}\frac{\partial h}{\partial z})+ j_r E_r+j_z E_z-R, \qquad (4)$$

Conservation of thermal energy:

$$\frac{\partial}{\partial t}(\rho C_p T)+\frac{u}{r}\frac{\partial}{\partial r}(\rho C_p rT)+w\frac{\partial}{\partial z}(\rho C_p T)= \frac{1}{r}\frac{\partial}{\partial r}(kr\frac{\partial T}{\partial r})+\frac{\partial}{\partial Z}(K\frac{\partial T}{\partial Z})-\frac{\Delta H}{C_P}\frac{\partial F_L}{\partial t} \quad (5)$$

Conservation of electrical charge:

$$\frac{1}{\mathrm{r}}\frac{\partial}{\partial \mathrm{r}}(\sigma \mathrm{r}\frac{\partial \phi}{\partial \mathrm{r}})+\frac{\partial}{\partial \mathrm{z}}(\sigma\frac{\partial \phi}{\partial \mathrm{z}})=0 \quad (6)$$

Current continuity equation:

$$\frac{1}{r}\frac{\partial}{\partial r}(rj_r)+\frac{\partial}{\partial z}(j_z)=0, \quad (7)$$

Ohm's law:

$$j_r=-\sigma E_{r,}\, j_z=-\sigma E_z \quad (8)$$

For boundary condition of fluid field:

$$\int_\Omega \partial P[\frac{1}{C^2}\ddot{P}+(\nabla)^Y\nabla P]d\Omega+ \int_{T_1}\partial P n^T\ddot{u}\,dT+\int_{T_3}\partial P\frac{1}{g}\ddot{P}\,dT=0 \quad (9)$$

For boundary condition of solid field:

$$\int_\Omega \partial u[P_s\ddot{u}+S^T DSu]d\Omega- \int_{T_1}\partial u^T\bar{t}\,dT=0 \quad (10)$$

Heat transfer equation:
For conduction :

$$q_X=-k_{xx}\frac{dT}{dx} \quad (11)$$

$$\frac{\partial}{\partial x}(k_{xx}\partial T/\partial x)+\partial/\partial y(k_{yy}\partial T/\partial y)+Q=0 \quad (12)$$

For convection:

$$q_h=h(T-T\infty) \quad (13)$$

$$\frac{\partial}{\partial x}(k_{XX}\partial T/\partial x)+Q= \rho C\frac{\partial T}{\partial t}+\frac{hP}{A}(T-T\infty) \quad (14)$$

Potential of heat transfer equation:

$$\Pi p=u+\Pi_V+\Pi_q+\Pi_h$$
$$\Pi_V=-\iiint_V QTdV,\pi_q=-\iint_{S_2}q+ds,$$
$$\pi_h=\frac{1}{2}\iint_{S_1}h(T-T\infty)^2\,dS \quad (15)$$

where t is the time, h the enthalpy, P the pressure, υ_z and υ_r the axial and radial components of velocity respectively, j_z and j_r the axial and radial component of the current density respectively, g the acceleration due to gravity, k the thermal conductivity, Cp the specific heat, ρ the density, η the viscosity, s the electrical conductivity, σ the radiation emission power, E_r and E_z the radial and axial components of the electric field defined by E_r= $-\partial V/\partial r$ and E_z= $-\partial V/\partial z$ and V is electric potential.

The azimuthal magnetic field B_θ induced by the arc current is evaluated by Maxwell's equation:

$$\frac{1}{r}\frac{\partial}{\partial r}=(rB_\theta)\mu_0 j_z,$$

where μ_0 is the permeability of free space.

In the solution of Eqs. (1)–(6), special attention needs to be put on the energy effects on the electrode surface. At the cathode surface, additional energy flux terms should be included in Eq. (4) because of thermionic cooling due to the mission of electrons, ion heating, and radiation cooling.

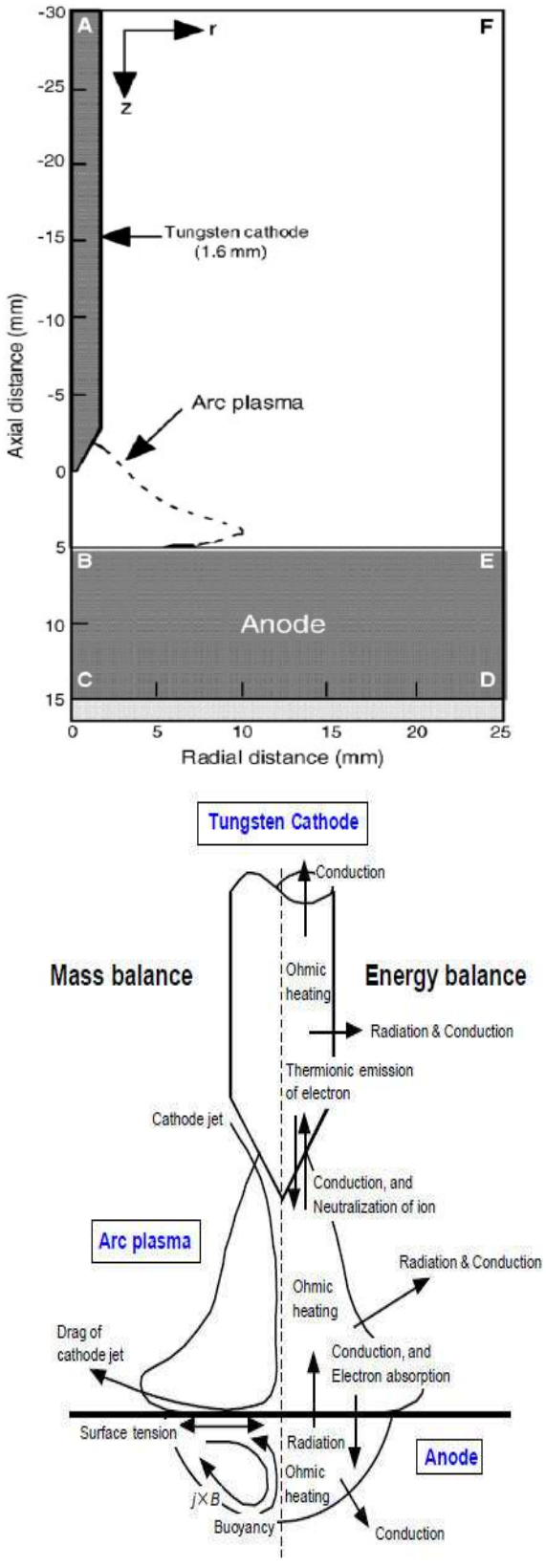

Fig.3.Schematic illustration of calculated domain.[2]

The additional energy flux for the cathode H_K is:

$$H_K = -\varepsilon\alpha T^4 - |\, j_e \,|\phi_K + |\, j_i \,|V_{i,} \qquad (16)$$

where ε is the surface emissivity, α the Stefan-Boltzmann constant, ϕ_k the work function of the tungsten cathode, V_i the ionization potential of argon, j_e the electron current density and j_i the ion current density. At the cathode surface, thermionic emission current of electron, j_e, cannot exceed the Richardson current density J_R [17] given by:

$$|j_R| = AT^2 \exp(-\frac{e\phi_e}{k_B T}) \qquad (17)$$

where A is the thermionic emission constant of the cathode surface, ϕ_e the effective work function for thermionic emission of the surface at the surface temperature and K_B the Boltzmann's constant. The ion-current density j_i is then assumed to be $|j|$-$|j_R|$ if $|j|$ is greater than $|J_R|$, where $|j|=|j_e|+|j_i|$ is the total current density at the cathode surface obtained from Eq. (5).

Similarly, for the anode surface, Eq. (4) needs additional energy flux terms for thermionic heating and radiation cooling. The additional energy flux for the anode H_A is:

$$H_A = -\varepsilon\alpha T^4 + |\, j \,|\phi_A, \qquad (18)$$

where ϕ_A is the work function of the anode and $|j|$ the current density at the anode surface obtained from Eq. (5).

The term including ϕ_A accounts for the electron heating on the anode because electrons deliver energy equal to the work function when being absorbed at the anode. The term is analogous to the cooling effect that occurs at the cathode when electrons are emitted. [4]

2.3 Materials models:

In the study that is done for solid, the isotropic model and for fluid the ideal fluid model is used.

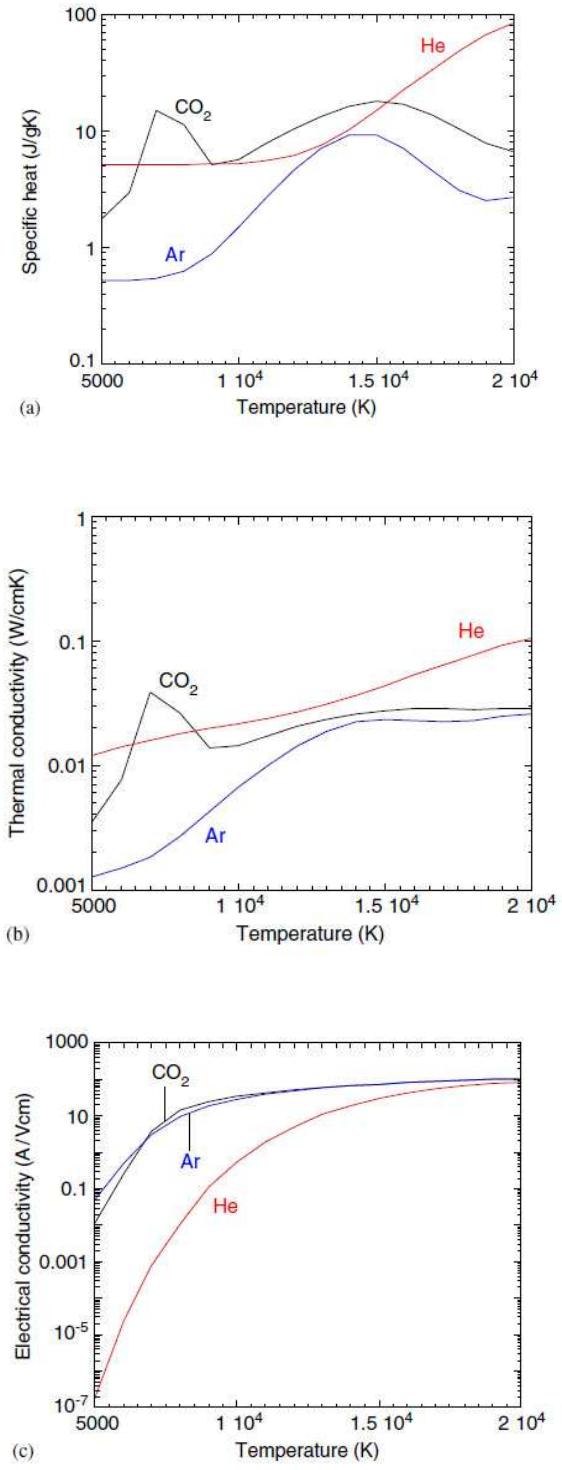

Fig.4.Dependences of specific heat, thermal conductivity and electrical conductivity of gases on temperature.
(a)Specific heat, (b)thermal conductivity and (c) electrical conductivity.[3]

2.4 Parameter Definition

For giving data to temperature and fluid velocity, that depend on time, the parameter is defined to the variation of this parameters since the GTAW machine is on till it is off and the workpiece cooling, is considered in the software.

2.5 Control Parameters

To control the outputs, the whole solution time and stopping of solution, the control parameters are used. This analysis was done in Two steps. First, Flotran setup. Second, FSI setup. In first step, the total solution time, 5 second and each step was defined 0.001. In second step, after defining nodes that have solid and fluid interface conditions, convergence rate is assumed to be 0.01. finally the replacing analysis assumed to be transmitted.[11]

2.6 Design Parameter

In coding, for GTAW optimization, the simulation design parameters are geometrical conditions of solid and fluid fields, standoff, nozzle angle, nozzle speed, temperature and pressure of environment and initial temperature of workpiece. Also the velocity and input temperature of plasma and shielding gases can be named as condition parameters.

3 Results and Discussion

Fig.5. shows two-dimensional distributions of the temperature and flow velocity in Ar, He and CO_2 GTA at 150A arc current.

The peak temperatures on the anode surface are 600, 1000 and 1200K, respectively for Ar, He and CO_2 GTA . The peak plasma temperatures and the flow velocities are 17000, 19000 and 25000 K, and 217, 298 and 748 m/s, respectively, while the arc voltages are 10.8, 19.9 and 17.3 V, correspondingly.

Fig.6. shows the radial distribution of heat input intensity onto the anode surface consisting of the heat transportation from electrons (enthalpy and condensation) and the heat conduction. The peak heat input intensities are 5000, 16 000 and 17 600 W/cm^2, respectively.

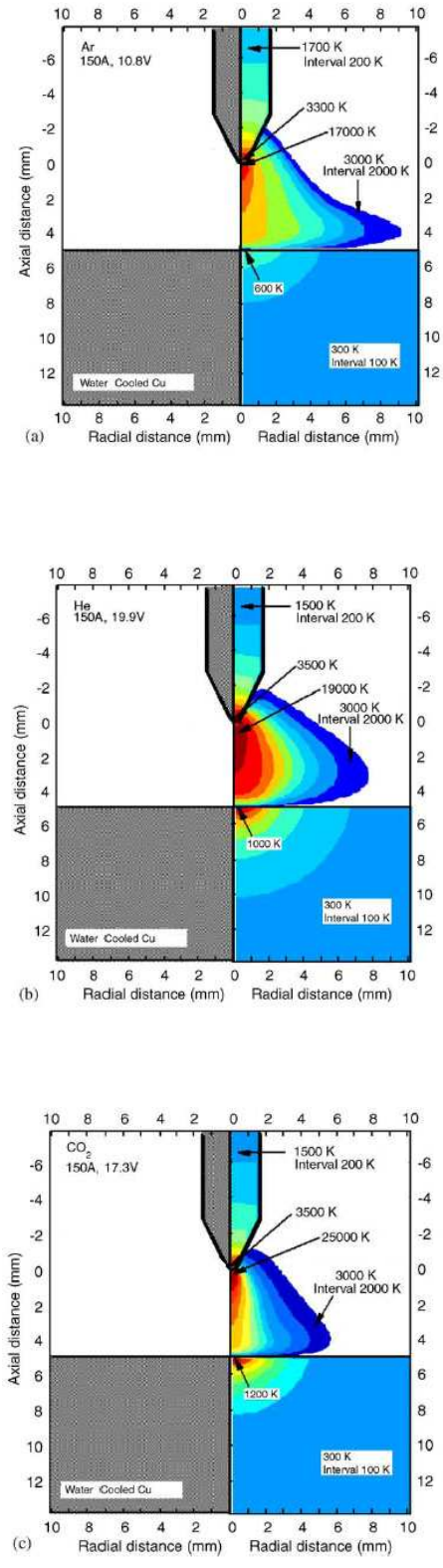

Fig.5. Two-dimensional distributions of temperature and flow velocity in argon, helium and carbon dioxide gas tungsten arc at 150A arc current.(a) Ar, (b) He, (c) CO_2[3]

For He GTA, the peak temperature on the anode surface reaches 1000 K, which is proximately two times higher than that of Ar GTA, mainly due to the higher peak of heat intensity caused by the current current constriction. As shown in Fig.4, the lower electrical conductivity of He than that of Ar reduces the diameter of the current channel and leads to the current constriction. The heat transportation from electrons is, therefore, concentrated near the arc axis. On the other hand, the plasma temperature and the flow velocity near the cathode are slightly higher than those of Ar GTA because of the high thermal conductivity of He.

Since the expansion of high-temperature region on the cathode surface leads to the arc root expansion, the increase in current density is suppressed and resultantly the temperature and the flow velocity are relatively low due to the low pinch force.

Now, turn to the results for CO_2 GTA. The peak temperature on the anode surface reaches 1200K that is slightly higher than that of He GTA. The heat transportation from electrons is comparable to that of He GTA, but the peak heat input intensity is higher than that of He GTA because the heat conduction in CO_2 GTA is higher due to the higher plasma temperature near the anode surface.

Fig.7. shows the radial distribution of current density on the anode surface. The peak current densities are 700, 2025 and 1875 A/ cm^2, respectively.

As shown in this Fig, the current channel in CO_2 GTA is also constricted. It is considered that the constriction is caused by the high mole specific heat of CO_2. The mass specific heat of CO_2 is nearly comparable to that of He, but mole specific heat is much higher than that of He due to the difference in molecular weights. The high mole specific heat will suppress the expansion of the high-temperature region in the plasma, and hence constrict the current channel near the cathode. The current constriction lifts the plasma temperature and the flow velocity due to the enhanced pinch force. The increased flow velocity prompts the energy loss in the fringe of the plasma, and hence the constriction of the plasma raises the arc voltage. As a result, the peak heat input intensity onto the anode increases.

Cooper temperature field is according to Fig.8,9. if the shielding gas be a mixture of Ar, He in which the transmission of produced heat to copper is shown completely .

Also the diagram of Fig.10. shows the temperature variations on loading surface.[4]

This diagram includes different parts that shows the way of heat transfer between source and shielding gas and the air around them.

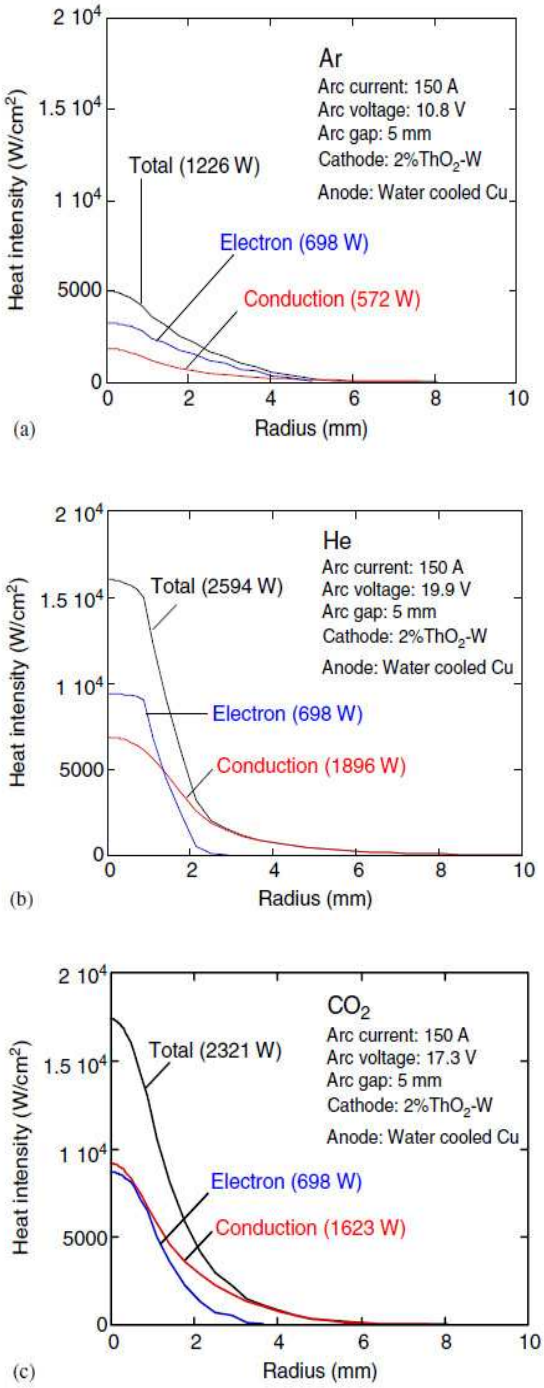

Fig.6. Radial distributions of heat intensity onto the surface of watercooled copper anode for argon, helium and carbon dioxide gas tungsten arc at 150A arc current. (a) Ar, (b) He, (c) CO_2[3]

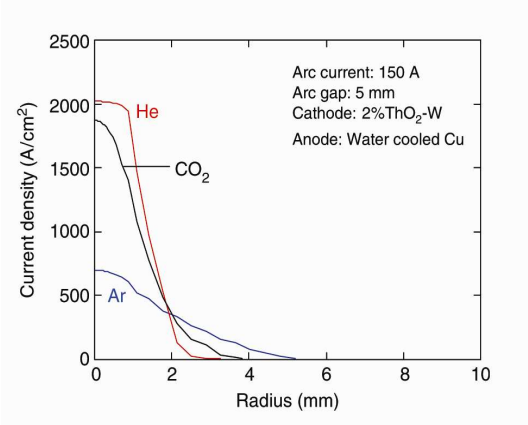

Fig.7. Radial distributions of current density onto the surface of watercooled copper anode for argon, helium and carbon dioxide gas tungsten arc at 150A arc current.[3]

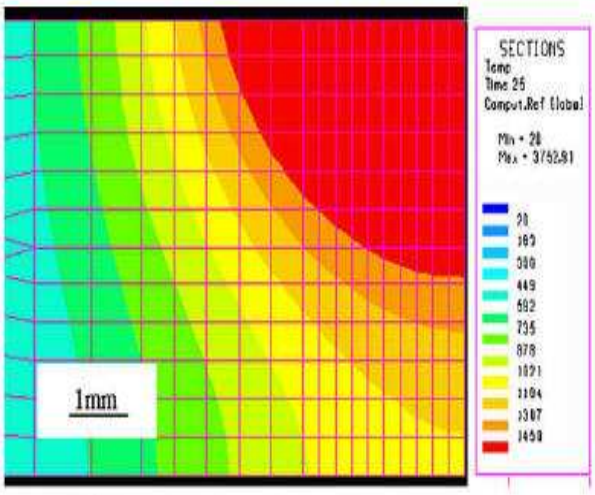

Fig.8.copper temperature field (Ar-He GTAW)[3]

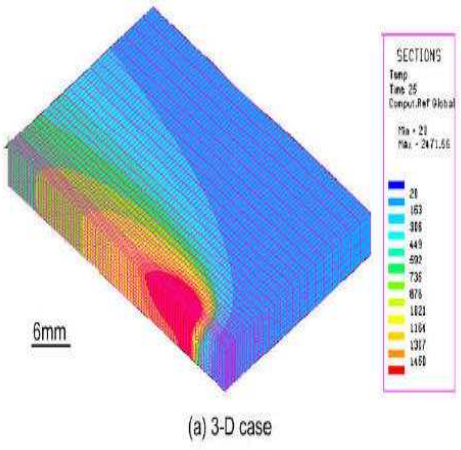

Fig.9.copper temperature field (Ar-He GTAW) -3D [3]

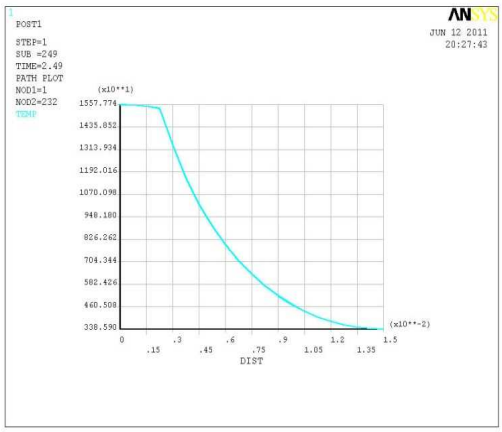

Fig.10.Temperature variations on loading surface [3]

4 Conclusions

The properties of the arc plasma and the heat input intensity onto the anode surface for CO2 GTA were numerically analyzed ignoring the oxidation of the electrodes. The results were compared with those of conventional Ar and He GTA. It was predicted that CO2 GTA would have excellent energy source properties approximately comparable to that of He GTA. The conclusions are summarized as follows.

(1) A molecular gas with high mole specific heat such as CO_2 has the ability to constrict arc plasma and hence increases current density near the arc axis. The peak current density of CO_2 GTA on the anode surface and the arc voltage are respectively 1875 A/ cm^2 and 17.3 V, comparable to those of He GTA.

(2) The peak plasma temperature and flow velocity near the cathode are respectively 25 000K and 748 m/s, which are much higher than those of Ar and He GTA and lead to high arc pressure.

(3) The peak heat input intensity onto the anode surface is 17 600W/cm^2, which is higher than those of Ar and He GTA. The intensity due to the heat transportation from electrons is 8400W/cm^2, which is comparable to that of He GTA. However the intensity due to the heat conduction is 9200 W/cm^2, which is higher than that of He GTA due to the high temperature of the CO_2 plasma near the anode surface.

(4)According to achieved results from numerical solution for all tree cases of shielding gas it is obvious GTAW process is suitable for cooper, because of the depth of weld diffusion compared with width and melting deficiency, is so high.

References

[1]Moarrefzadeh.A, Numerical simulation of copper temperature field in GTAW process, WSEAS conference, Hangzhou, 11-13 April 2010

[2] Inaba T, Iwao T. IEEE Trans Dielectr Electr Insul 2000;P.684–92.

[3]Ansys Help system, Analysis Guide & Theory Reference , Ver 9,10

[4]Gorman,E."New developments and application TIG welding"Welding journal, July 2004,P.547-556 .

[5]Wang,Y., Chen,Q."On-line quality monitoring in TIG arc welding" Journal of Materials Processing Technology, January 2005,P.270-274

[6]Kyselica,S."High–Frequency reversing arc switch for GTAW process of Aluminum "Welding journal, May 2005, P.31-35.

[7] Patanker SV. Numerical heat transfer and fluid flow. Washington, DC: Hemishpere; 1980.

[8] P.fender E. Electric arcs and arc gas heaters. In: Hirsh MH, Oskam HJ, editors. Gaseous electronics. NewYork: Academic Press; 1978. P. 291–398

[9]Filipsky,S.P."Automated plasma arc keyhole welding for aerospace fabrication "Welding journal, June 2005,P439-501 .

[10]Martikainen,J."Conditions for achieving high-quality welds In GTAW of stainless steel" Journal of Materials Processing Technology, May 2005, P68-75

[11] Hyundai Heavy Industries Co., " Robot Operation Manual", WSEAS Edition, April 2002.

[12] J. Weigmann, G. Kilian, " Decentralization with ProfiBus DP/DPV1", Vol. 1, WSEAS Edition, April 2003.

[13]YUE HONG, SUN LIXIN, DAI SHIJIE . "Research on the Model of Arc Noise in Welding Seam Tracking", Proceedings of the 6th WSEAS International Conference on Simulation, Modeling and Optimization, Lisbon, Portugal, September 22-24, 2006.

[14] KHADIJEH DAEINABI, MOHAMMAD TESHNEHLAB. "Seam Tracking of Intelligent Arc Welding Robot " Proceedings of the 6th WSEAS Int. Conf. on Systems Theory & Scientific Computation, Elounda, Greece, August 21-23, 2006 (pp161-166)